recycling

MDPI

Article

Utilization of Mill Scale Waste as Natural Fine Aggregate Replacement in Mortar: Evaluation of Physical, Mechanical, Durability, and Post-Fire Properties

Apinun Siriwattanakarn [1], Ampol Wongsa [1], Nawapak Eua-Anant [2], Vanchai Sata [1,*], Piti Sukontasukkul [3] and Prinya Chindaprasirt [1,4]

[1] Sustainable Infrastructure Research and Development Center, Department of Civil Engineering, Faculty of Engineering, Khon Kaen University, Khon Kaen 40002, Thailand; apinun.s@kkumail.com (A.S.); ampowo@kku.ac.th (A.W.); prinya@kku.ac.th (P.C.)
[2] Department of Computer Engineering, Faculty of Engineering, Khon Kaen University, Khon Kaen 40002, Thailand; nawapak@kku.ac.th
[3] Construction and Building Materials Research Center, Department of Civil Engineering, Faculty of Engineering, King Mongkut's University of Technology North Bangkok, Bangsue, Bangkok 10800, Thailand; piti.s@eng.kmutnb.ac.th
[4] Academy of Science, Royal Society of Thailand, Dusit, Bangkok 10300, Thailand
* Correspondence: vancsa@kku.ac.th

Abstract: The current paper presents the findings from experiments focused on using mill scale waste (MSW) as a natural fine aggregate (NFA) replacement in making cement mortar, aiming to recycle this material. Mortars were prepared by mixing with ordinary Portland cement, NFA, and water. NFA was replaced with 5%, 10%, 15%, and 20%vol of MSW. The physical and mechanical properties of mortars including compressive and flexural strengths, density, porosity, water absorption, ultrasonic pulse velocity, thermal conductivity, durability properties, and characteristics after being subjected to elevated temperatures at 400, 700, and 1000 °C were investigated after 28 days of curing. The results showed that 15% MSW exhibited optimum compressive and flexural strengths. Also, the MSW mortar showed reduced workability and thermal conductivity, while the porosity slightly increased. The addition of MSW enhanced chloride resistance and mortar's residual compressive strength after exposure to various temperatures. These findings confirmed that MSW can be used as a sustainable fine aggregate to produce mortar with optimum physical, mechanical, durability, and post-fire properties.

Keywords: mill scale; waste; mortar; corrosion; fire-exposed

check for updates

Academic Editors: Bingxiang Yuan, Waseim Ragab Azzam, Binbin Yang and Shiyuan Huang

Received: 20 December 2024
Revised: 2 February 2025
Accepted: 3 February 2025
Published: 5 February 2025

Citation: Siriwattanakarn, A.; Wongsa, A.; Eua-Anant, N.; Sata, V.; Sukontasukkul, P.; Chindaprasirt, P. Utilization of Mill Scale Waste as Natural Fine Aggregate Replacement in Mortar: Evaluation of Physical, Mechanical, Durability, and Post-Fire Properties. *Recycling* **2025**, *10*, 20. https://doi.org/10.3390/recycling10010020

Copyright: © 2025 by the authors. Licensee MDPI, Basel, Switzerland. This article is an open access article distributed under the terms and conditions of the Creative Commons Attribution (CC BY) license (https://creativecommons.org/licenses/by/4.0/).

1. Introduction

Iron and steel making processes consume a substantial quantity of natural resources, particularly iron ore and coal. The steel industry produces around 600 kg of solid waste per ton of steel, including mill scale, sludge, and dust, some of which have a high iron concentration [1]. Most of these wastes are destined to be disposed of in landfills, although a sizeable portion of them can already be recycled within the company or utilized as co-products by other industrial sectors [2,3]. Mill scale is a residual product formed as a layer of iron oxide on the surface of steel during the continuous casting and rolling mill process. This occurs when the steel is exposed to varying temperatures in the presence of oxygen, which stimulates the formation of the iron oxide layer. The chemical composition of the mill scale depends on the specific type of steel manufactured and the method of production

utilized. Typically, there is 70% iron content, with trace quantities of non-ferrous metals and alkaline chemicals. It also contains wüstite (FeO), hematite (Fe_2O_3), and magnetite (Fe_3O_4) [4]. Only a portion of the mill scale can be reused during the sintering process at integrated steel plants [5].

To develop environmentally friendly materials, the usage of waste aggregates and mill scale in civil engineering applications has been looked into. Chousidis et al. [6] investigated the substitution of cement with mill scale at 5% and 10% by weight in concrete. Their study revealed that incorporating mill scale improved compressive strength and enhanced durability against chloride infiltration of concrete. Furthermore, the presence of mill scale in concrete resulted in a decrease in the level of chloride ions in cement mortars partially submerged in sodium chloride solution. Ismail and Al-Hasmi [7] replaced a portion of waste iron as a partial replacement of sand in concrete at 10%, 15%, and 20%. They conducted tests to evaluate the uniformity, density, compressive strength, and tensile strength of the concretes. The results showed that employing waste iron reduced consistency while the density, compressive strength, and flexural strength were enhanced. Alwaeli and Nadziakiewicz [8] substituted steel chips and scales as a partial replacement for sand in concrete at 25%, 50%, 75%, and 100% by weight of sand. Their investigation indicated that the concrete mixed with steel chips had better strength than conventional concrete, while the strength decreased in the case of concrete mixed with over 25% steel scale. They suggested that the use of steel chips and scales could be used for buildings as shielding concretes against gamma radiation. In addition, others reported that substituting a portion of natural sand with steel scale waste in mortar or concrete resulted in enhanced mechanical properties as well as durability [9,10]. However, research on the effect of high temperatures on mortar containing mill scale as fine aggregate is very limited.

The objective of this study was to examine the physical and mechanical properties of cement mortar containing MSW as fine aggregate. The properties of mortar, including its workability, compressive strength, flexural strength, density, porosity, water absorption, ultrasonic pulse velocity, thermal conductivity, and durability, were investigated. In addition, the characteristics of mortar after being subjected to elevated temperatures were evaluated. These results will facilitate the utilization of this waste in the production of eco-friendly cementitious material.

2. Materials and Methods

2.1. Materials

Ordinary Portland cement (OPC) with chemical composition of 63.1% CaO, 17.2% SiO_2, 4.0% Al_2O_3, 3.1% Fe_2O_3, 3.9% SO_3, 0.6% MgO, and 0.9% LOI (loss on ignition) and specific gravity of 3.15 was used. Natural fine aggregate (NFA) with a maximum size of 4.75 was used. Mill scale waste (MSW) originating from the rolling mill operation process was collected from a local factory (as shown in Figure 1). The MSW was washed, dried, and sieved by passing a 4.75 mm mesh. The major composition was 99.2%Fe_2O_3. To prevent any effect of the mortar on the free water content, NFA and MSW were used for mixing in a saturated surface-dry condition as per ASTM C128-22 [11]. The particle size distribution of fine aggregates was assessed using sieve analysis following ASTM C136-06 [12].

Figure 2 shows the physical attributes of the fine aggregates, while Figure 3 provides scanning electron microscope (SEM) images. Table 1 presents the physical characteristics of the fine aggregates. The specific gravity of MSW (5.52) exceeded that of NFA (2.60), but their unit weights were comparable. This similarity arose from the flat, thin, and irregular shapes of MSW (Figures 2 and 3), which increased void volume and lowered its unit weight. Figure 4 illustrates the particle size distributions of the fine aggregates. It shows that NFA's particle size distribution nearly adhered to the lower and upper limits specified by ASTM

C33/C33M-11 [13]. In contrast, MSW fell outside this range due to flat–thin and irregular particles received directly from the factory without any modification.



Figure 1. Mill scale waste at landfills.

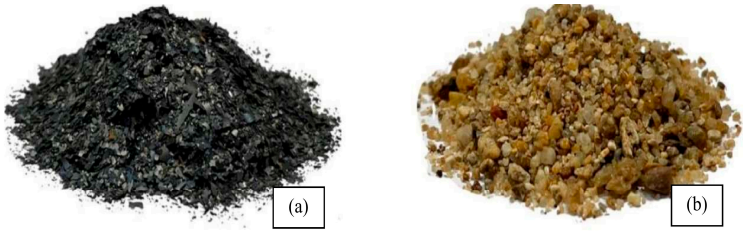


Figure 2. Physical characteristics of (**a**) MSW and (**b**) NFA.

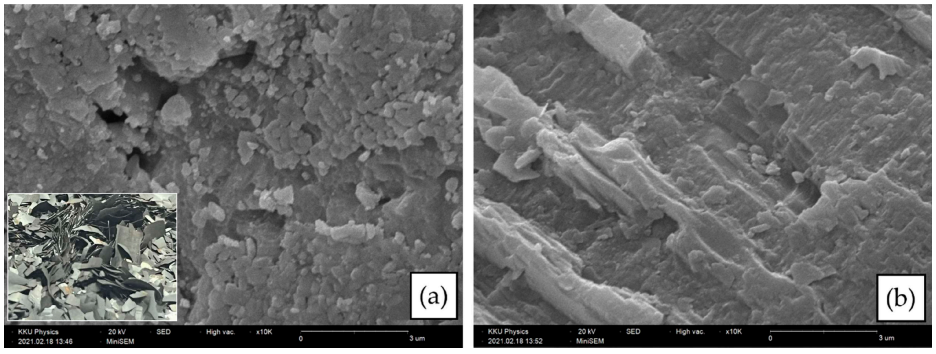


Figure 3. SEM images of the surface of fine aggregates: (**a**) MSW; (**b**) NFA.

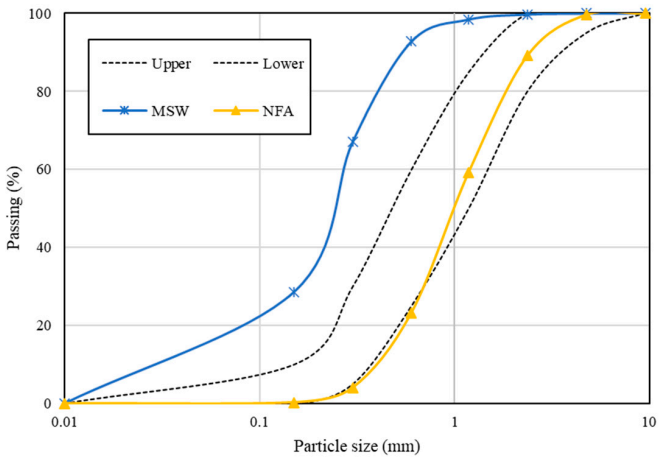


Figure 4. Particle size distributions of MSW and NFA.

Table 1. Physical properties of NFA and MSW.

Properties	NFA	MSW
Specific gravity	2.60	5.52
Fineness modulus	3.2	1.1
Unit weight (kg/m^3)	1636	1670
Water absorption (%)	0.95	0.04

2.2. Mix Proportions and Specimen Preparation

Five different mixes of cement mortar, labeled CM00, CM05, CM10, CM15, and CM20, were developed to represent mixes containing 0%, 5%, 10%, 15%, and 20% of MSW by volume of fine aggregate, respectively. Concerns about workability and maintaining the constant W/C of all mortar mixtures from pretesting the rate of NFA replacement by MSW in this study was limited to 20%. A water-to-cement ratio of 0.55 and an aggregate-to-binder ratio of 2.75 were used. The cement mortar mix proportions are shown in Table 2. The mixing procedure for the cement mortar was conducted following ASTM C305-11 [14]. After completing the mixing process, the specimens were prepared, then covered with cling film, and left undisturbed for 24 h. Following this, the specimens were removed from the molds and cured in limewater.

Table 2. Mix proportions of mortar (kg/m^3).

Title 1	OPC	NFA	MSW	Water
CM00	520	1430	0	286
CM05	520	1359	152	286
CM10	520	1287	304	286
CM15	520	1216	455	286
CM20	520	1144	607	286

2.3. Method of Testing

The workability of the fresh mortar was assessed following ASTM C1437-07 [15]. Mortar cubes sized 50 × 50 × 50 mm^3 were prepared to assess their compressive strength as per ASTM C109/C109M-13 [16]. In addition, these cubes were utilized to investigate density, porosity, and water absorption following ASTM C642-12 [17]. Furthermore, their resistance to sulfuric acid was evaluated following ASTM C267-13 [18]. The 40 × 40 × 160 mm^3 sample was used for the flexural strength test according to ASTM C348-22 [19]. The 100 × 100 × 100 mm^3 cube was used for the ultrasonic pulse velocity (UPV) test as per ASTM C597-08 [20], and the thermal conductivity was determined using ISOMET2114 [21] following ASTM D5930-09 [22].

The chloride penetration depth in the cement mortar was monitored over three months. The cylindrical specimens, with a diameter and height of 100 mm, were coated with epoxy resin, except for the bottom surface, which was left unsealed to permit diffusion. These specimens were submerged in a 3% sodium chloride (NaCl) solution. During the testing, a 0.1 N silver nitrate ($AgNO_3$) solution was sprayed on the freshly cut surface of the specimens. The reaction between $AgNO_3$ and NaCl resulted in a visible silver-white color [23].

The surface resistivity measurement was conducted using a commercially available 4-point Wenner probe surface resistivity meter [24]. The mortar samples were in a saturated surface-dry (SSD) condition at a temperature of 23 ± 2 °C. Measurements were conducted twice, capturing the circular face of each mortar cylinder at angles of 0, 90, 180, and 270 degrees. The results in this study were gathered utilizing a probe spacing of 38 mm (1.5 inches). The apparatus quantifies the electric current passing through the outside

electrodes and the voltage difference across the two inner electrodes. A bulk resistivity test was conducted on the identical cylindrical sample used for the surface electrical resistivity measurement. The test yielded a response in a mere 2 seconds, while the entire process of sample preparation and testing was completed in under 30 min. The conductivity of a fully saturated mortar specimen indicates the mortar's resistance to the entrance of ionic species through the diffusion mechanism.

The post-fire behavior of the mortar was investigated by subjecting the samples to gradual heating in an electric furnace. The temperature was increased at a rate of 3–5 °C per minute [25]. Upon reaching target temperatures of 400, 700, and 1000 °C, they were maintained for 2 h. Subsequently, the samples were allowed to cool in the furnace and then underwent compressive strength tests to assess their remaining strength.

A summary of testing details is shown in Table 3.

Table 3. Summary of testing details.

Properties	References	Shapes and Dimensions	Age at Testing (Days)
Workability	ASTM C1437 [15]	-	Fresh mortar
Compressive strength	ASTM C109 [16]	Cube, 50 × 50 × 50 mm^3	7 and 28
Density, porosity, and water absorption	ASTM C642 [17]	Cube, 50 × 50 × 50 mm^3	28
Sulfuric acid resistance	ASTM C267 [18]	Cube, 50 × 50 × 50 mm^3	7, 14, 28, 56, 90, 120, and 180
Flexural strength	ASTM C348 [19]	Prism, 40 × 40 × 160 mm^3	28
Ultrasonic pulse velocity	ASTM C597 [20]	Cube, 100 × 100 × 100 mm^3	28
Thermal conductivity	Wongkvanklom et al. [21], ASTM D5930 [22]	Cube, 100 × 100 × 100 mm^3	28
Chloride penetration depth	Otsuki et al. [23]	Cylindrical, ø 100 mm × 100 mm	28, 56, and 90
Surface and bulk resistivity of mortar	Ghosh and Tran [24]	Cylindrical, ø 100 mm × 200 mm	7, 28, and 90
Post-fire behavior of cement mortar	Wongsa et al. [25]	Cube, 50 × 50 × 50 mm^3	28

3. Results and Discussion

3.1. Flow Value

Figure 5 presents the workability of the fresh mortar mixes determined by the flow table test. As the proportion of MSW increased, the flow of fresh mortar declined, from 140% for CM00 mortar to 20% for CM20 mortar. This finding is consistent with previous research showing that replacing NFA with finer particles caused a reduction in workability [26]. As the percentage of fine particles increased, the workability decreased. In this study, the fineness modulus of the MSW was 1.1, which was lower than that of NFA (3.2), as shown in Table 1 and Figure 4. In addition, the considerable reduction in the flow value could be attributed to the flat–thin and irregularly shaped particles and the rough surface of MSW (Figures 2 and 3), which negatively contributes to the ball-bearing effect and results in workability reduction [26].

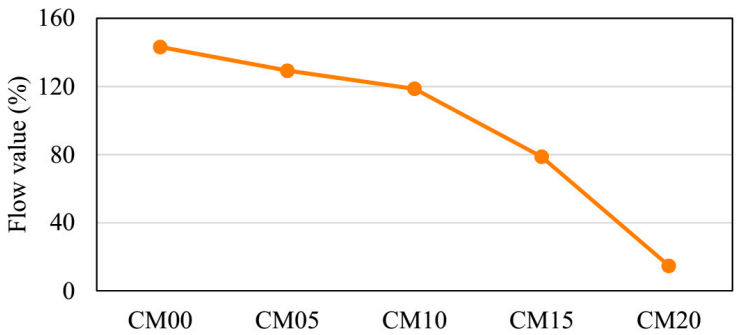


Figure 5. Flow values of fresh mortars.

3.2. Compressive and Flexural Strengths

Figure 6 illustrates the compressive strength values of mortar specimens. The mortar sample containing 5–10% MSW displayed lower compressive strength compared to the plain mortar sample (CM00) due to the increase in porosity. However, it was noted that the increase in compressive strength was contingent on the substitution ratio. The highest compressive strength at 28 days was 44.1 MPa at a substitution ratio of 15% (CM15), which was higher than that of plain mortar (42.0 MPa). Figure 7 shows the flexural strength of mortar specimens that included MSW at different ratios. Observations revealed that the flexural strength varied by the MSW ratio. The flexural strength increased proportionally with the substitution ratio, ranging from 5% to 20%. Many reports [6,9,10,27] have claimed that the use of MSW as fine aggregate can improve the strength of the mortar or concrete samples. It was discovered in the current investigation that owing to the uneven structures of the MSW (as seen in Figure 3), the improvement in compressive strength of the mortar containing the MSW depended on the replacement ratio. The increase in MSW content at 15% seemed to enhance the compressive and flexural strengths, mostly because of the denser microstructure, rougher surface, and elongation of MSW particles, as well as the better interfacial transition zone (ITZ). At 28 days, the compressive strength had increased by about 5% and the flexural strength by about 40% compared with the control mortar. However, at the high MSW content (20%), the cement mixture is thought to have leaked between the irregular structures of the MSW. As a result, an immovable interlocking was created between the MSW and the cement paste. Compaction and homogeneous mixing of the slurry were inhibited by the reduction in workability. A decline in compressive strength at high MSW replacement has also been seen as the phenomenon's consequence [28].

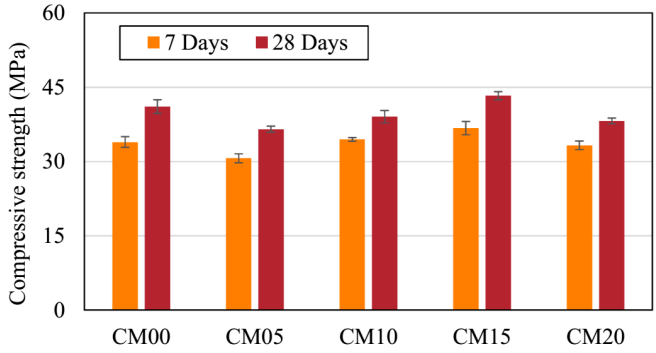


Figure 6. Compressive strength of mortars.

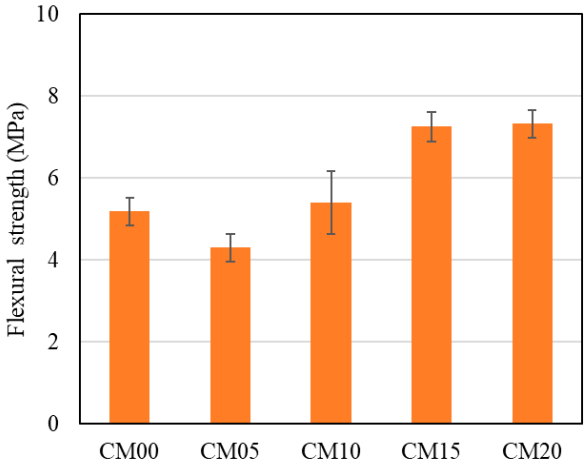


Figure 7. Flexural strength of mortars at 28 days.

3.3. Dry Density, Porosity, Water Absorption, Thermal Conductivity, and Ultrasonic Pulse Velocity

Table 4 shows a summary of the test findings for the mortar's dry density, water absorption, porosity, thermal conductivity, and ultrasonic pulse velocity. Dry density measurements ranged from 2134 to 2371 kg/m^3, with porosity values slightly increasing between 17.38% and 18.10%. The mortar containing MSW demonstrated increased density compared to conventional mortar due to the high specific gravity of MSW (5.52). The porosity slightly increased as the proportion of MSW replacement increased, which can be attributed to the flat–thin and irregularly shaped particles of MSW compared to NFA. This caused the texture of the mortar to be rather dry, as shown by the workability in Figure 5, and led to an increase in porosity. The water absorption values of mortar containing MSW varied in a narrow range from 7.83% to 8.71%. The water absorption value decreased with increasing amounts of MSW content. Since the water absorption of MSW was very low (0.04%), as shown in Table 1, the water absorption seemed to be little decreased, even though the porosity increased.

Table 4. Density, porosity, water absorption, thermal conductivity, and ultrasonic pulse velocity of mortar.

Mix	Density (kg/m^3)	Porosity (%)	Water Absorption (%)	Thermal Conductivity (W/m-K)	Ultrasonic Pulse Velocity (m/s)
CM00	2134	17.38	8.71	1.58	3390
CM05	2106	17.50	8.66	1.47	3400
CM10	2192	17.90	8.54	1.45	3590
CM15	2368	17.88	8.01	1.42	3470
CM20	2371	18.10	7.83	1.36	3450

The thermal conductivity of the cement mortar ranged from 1.36 to 1.57 W/m-K. The thermal conductivity of mortar containing MSW as a fine aggregate replacement was related to the porosity. Figure 8 shows the relationship between porosity and thermal conductivity. As the porosity of cement mortar increased, the thermal conductivity values decreased. Previous reports [29–32] have also established a correlation between thermal conductivity and residual porosity. Sornlar et al. [33] indicated that the thermal conductivity was influenced by the total porosity, rather than the open and closed porosity. Furlani and Maschio [34] also demonstrated that an increase in MSW content led to a decrease in thermal conductivity compared to the reference cement mortar.

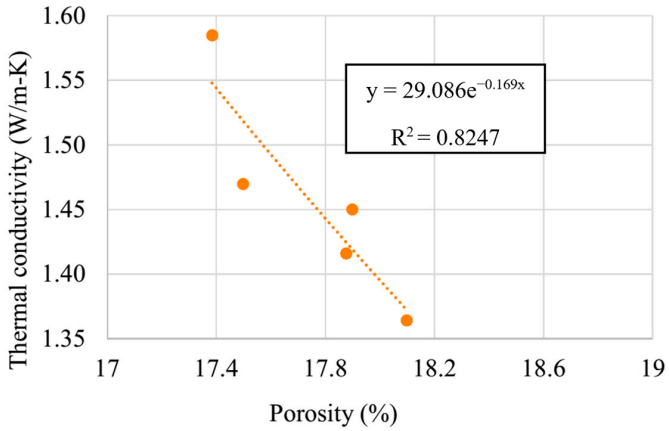


Figure 8. Relationship between thermal conductivity and porosity of mortar.

The ultrasonic pulse velocity (UPV) test is recognized as a vital method for evaluating the mechanical and physical properties of cement-based materials, with a clear correlation observed between UPV levels and compressive strength [35]. As indicated in Table 4,

the pulse velocity of the mortar samples ranged from 3390 m/s to 3590 m/s. Notably, the UPV values of the mortars exhibited an increase with the steel scale content in the samples. The highest UPV value was obtained at 10–15% of the MSW substituted with NFA. The transmission of the ultrasound was influenced by the surrounding environment through which the pulse travels. A dense medium occurred due to the strong adhesion between the cement paste and MSW. Therefore, the increase in MSW of mortar mixtures resulted in a rising ultrasonic pulse velocity, since the velocity of ultrasonic pulses was faster in a denser environment. Furthermore, the UPV increment observed in the mortars when increasing the MSW content may be attributed to the higher bulk density of the MSW than the NFA [9]. Figure 9 compares the compressive strength and UPV of mortar at 28 days. The results indicate that adding 5–10% MSW increased UPV, likely due to MSW enhancing pulse transmission. However, increasing MSW to 15–20% decreased UPV because of higher porosity. The compressive strength of the mix with 5% MSW was slightly lower, but increased trends were observed with 10–15% MSW before declining at higher contents. The relationship between UPV and compressive strength was unclear, potentially due to the effects of porosity and differences in properties of NFA and MSW. This suggests that additional factors should be considered when using UPV to estimate compressive strength [36].

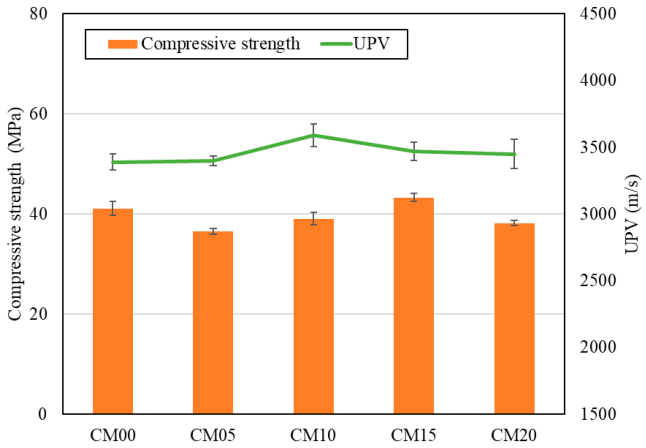


Figure 9. Comparison of compressive strength and UPV of mortar.

3.4. Sulfuric Acid Resistance

Figure 10 illustrates the percentage of weight reduction for samples subjected to sulfuric acid solution. After being exposed to 3% sulfuric acid for 28 days, every cement mortar exhibited a slight weight change. However, after being immersed for 90 days, a considerable loss in weight was observed. This phenomenon arose due to the presence of calcium hydroxide and other calcium compounds, which are byproducts of cement hydration. As demonstrated by Nuaklong et al. [37], sulfuric acid readily degrades these calcium compounds. When exposed to sulfuric acid, the cement mortar underwent a chemical reaction with the calcium hydroxide (C–H) and calcium silicate hydrate (C-S-H) compounds, leading to the formation of calcium sulfoaluminate (ettringite, AFt) and calcium sulfate (gypsum). This reaction resulted in specimen expansion, splitting, and weight loss. In this study, the rise in MSW content did not seem to impact the ability to resist corrosion. The weight loss values of all mixtures exhibited only marginal disparities, which ranged between 75% and 82% at 180 days of corrosion. Extended exposure for 180 days in 3% concentrated sulfuric acid caused significant deterioration of the samples, and a high weight loss of more than 80% was observed. These results are in line with Parvathikumar et al. [38] work, which studied the durability of concrete with MSW to

partially replace fine aggregate and found that the weight loss due to sulfuric acid attack seemed to increase with MSW replacement.

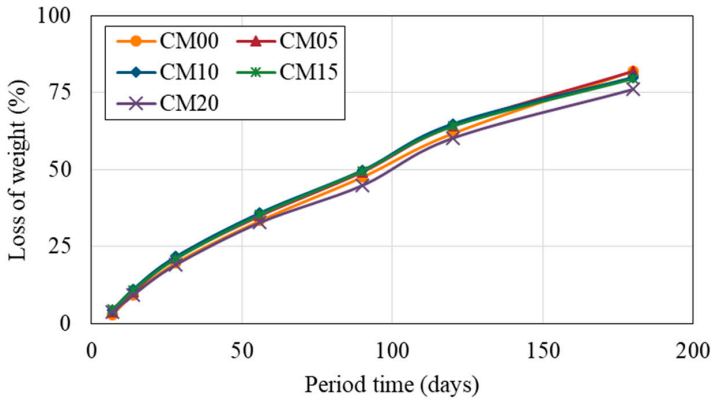


Figure 10. Loss of weight after acid exposure to mortar.

3.5. Chloride Penetration Depth

Figure 11 illustrates the split surfaces of specimens' immersion in a 3% NaCl solution after the application of a 0.1 N silver nitrate solution. A notable disparity in the chloride ion penetration depths was observed between mortars incorporating MSW and those composed of NFA, exhibiting significantly reduced penetration depths across all immersion durations.

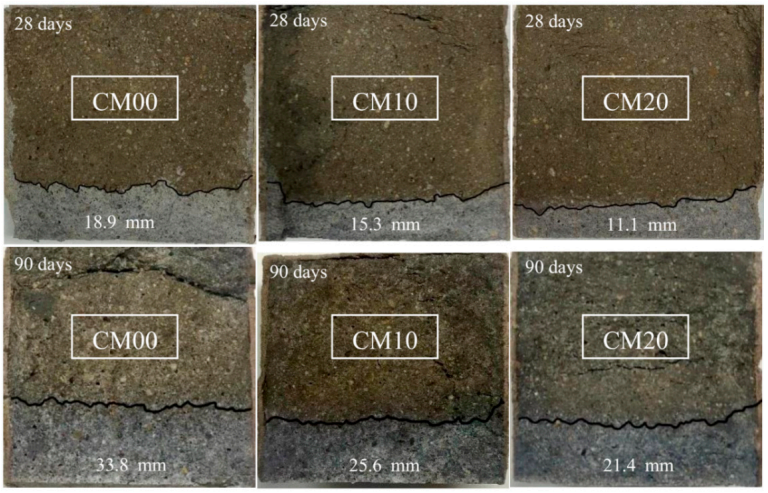


Figure 11. The visual appearance of mortar after immersion in NaCl solution for 28 and 90 days.

Figure 12 shows the depth of chloride penetration for periods of 28, 56, and 90 days. For the replacement of NFA by MSW in mortar, the results indicate that the resistance to chloride penetration was superior in comparison to the plain mortar. This may be due to calcium hydroxide from the hydration reaction and the presence of iron oxides in the MSW reaction to create more C-S–H gel [27]. The permeability decreased as the C-S–H gel filled the concrete pores [38]. The most effective in this experiment was achieved by substituting 20% of NFA with MSW. The chloride penetration depths of CM00 were observed to be 18.9 mm and 33.8 mm after immersing the material in a 3% NaCl solution for 28 and 90 days, respectively. CM05, CM10, CM15, and CM20 displayed 28-day chloride penetration depths of 16.2 mm, 15.3 mm, 14.0 mm, and 11.1 mm, while at 90 days, these were 27.5 mm, 25.6 mm, 23.2 mm, and 21.4 mm, respectively. Furthermore, the depth of chloride penetration in all cement mortar samples exhibited a consistent and gradual increase throughout the entire duration of the soaking period, culminating after the test. As

an example, the depth of chloride penetration in CM20 was initially measured at 11.1 mm after 28 days of immersion, and it increased to 24.1 mm after 90 days of immersion.

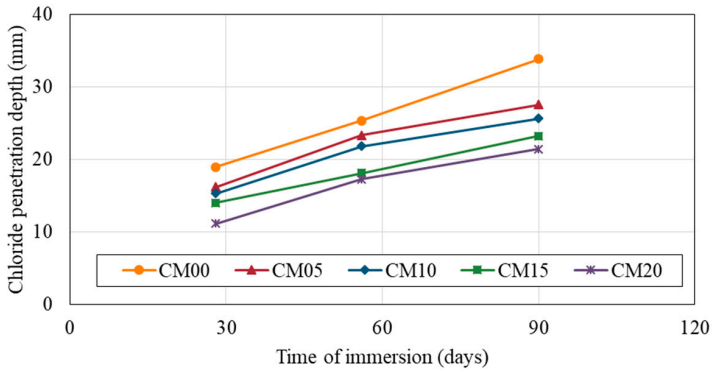


Figure 12. Chloride penetration depth of cement mortar.

3.6. Surface and Bulk Resistivity of Mortar

Electrical resistivity is a non-destructive testing method and can evaluate the microstructure of concrete and be utilized to predict the diffusion coefficients of chloride ions [24,39]. Figures 13 and 14 illustrate that the inclusion of MSW in the mortar matrix had a significant effect on resistivity in comparison to NFA. Both the surface and bulk resistivity exhibited a nearly linear increase as the MSW content rose from 0% to 20%. For 0% MSW content mortar (CM00), the surface resistivity at 7, 28, and 90 days was 3.7, 4.33, and 5.1 kΩ·cm, which increased to 4.3, 5.2, and 5.9 kΩ·cm for 10% MSW content (CM10) or increased about 14.1%, 18.7%, and 17.5%, respectively. The 28-day surface resistivity and bulk resistivity increased from 4.3 to 5.6 kΩ·cm and 3.0 to 3.8 kΩ·cm, respectively, as the content of the MSW content increased from 0% to 20%. This showed that the addition of MSW to the cement mortar mixture enhanced its ability to resist chloride penetration and improved its electrical resistance. The results are similar to the chloride penetration depth tests described above. Ganeshprabhu et al. [27] studied the use of MSW as sand replacement in concrete production and claimed that the rough surface texture and high angularity of MSW particles increased bonding capacity with cement, thus producing very dense concrete. This may enhance chloride penetration resistance and also its mechanical properties. In addition, Chousidis et al. [6] and Parvathikumar et al. [38] also found that including MSW in the concrete mixture could improve the durability of the cementitious composites against chloride infiltration. Furthermore, the results showed that at the same condition, the surface resistivity was higher than that of bulk resistivity, which showed the same trend as other studies [24,40].

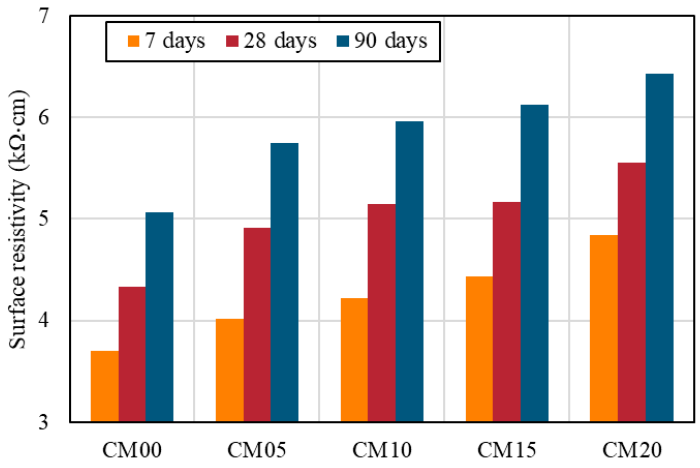


Figure 13. Surface resistivity of cement mortar.

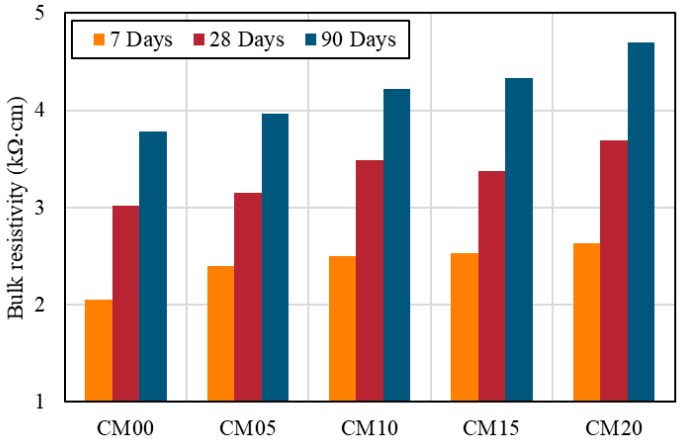


Figure 14. Bulk resistivity of cement mortar.

This study showed that incorporating MSW in mortar improved chloride resistance, electrical resistivity, and acid resistance, despite the higher porosity compared with control mortar. Replacing NFA with MSW at levels of 5–20% had a greater effect on corrosion resistance than the increase in porosity. Additionally, the slight increase in porosity of 0.72% (from 17.38% to 18.10%) is unlikely to significantly impact corrosion resistance.

3.7. Post-Fire Behavior of Cement Mortar

3.7.1. Appearance Changes

The deterioration of concrete due to high temperature can be identified by visually observing changes in its color and appearance [41–43]. Under normal conditions, all mortar samples exhibited a gray color. As shown in Figure 15, upon exposure to a temperature of 400 °C, the color changed to a light gray. This alteration occurred as a result of the dissolution of ettringite, leading to the release of some chemically bound water. Subsequent exposure to a temperature of 700 °C resulted in a yellowish gray due to the presence of Fe_2O_3 in the cement and MSW. At this temperature, the complete decomposition of ettringite occurred along with the release of a larger quantity of chemically bound water. Finally, when exposed to a temperature of 1000 °C, the products become yellowish brown as the content of Fe^{3+} increased [42].



Figure 15. Color and appearance changes of mortar after exposure to elevated temperatures.

In addition, there were no visible fissures on the surface of the samples following exposure to a temperature of 400 °C. At temperatures equal to or more than 700 °C, visible surface cracks were discovered at the MC00 and MC05 mortar surfaces. The fissures became notably visible after exposure to temperatures of 700 °C and 1000 °C, particularly in mortar containing a low MSW content. However, CM15 and CM20 mortars showed fewer and fewer cracks. Understanding this phenomenon requires recognizing that cracks were induced by heat stress within the mortar. Therefore, reducing this stress is essential for mitigating cracks. Substituting NFA with MSW in mortar caused a considerable increase in porosity and a decrease in the thermal conductivity of the mortar, which resulted in reduced thermal strain.

3.7.2. Weight Loss

The impact of increased temperatures on the weight loss of mortar is shown in Figure 16. These results indicate that when the temperature was raised, the weight loss increased. Furthermore, it can be inferred that the reduction in weight of the mortar primarily took place between the normal temperature and 700 °C. The weight of mortar after exposure ranged from about 94.5% to 98.5% of the initial weight at all temperature ranges. It has been observed that weight loss exhibits a minimal rise with rising temperature. The primary cause of this phenomenon is the process of water evaporation. The capillary and gel water constitute a significant proportion of the volume of cement paste and are expected to evaporate before reaching a temperature of 400 °C. Chemically bound water, integral to hydration products, evaporates at elevated temperatures. This evaporation contributes to the observed weight loss up to a temperature of 1000 °C [42]. At temperatures of 400 °C, the weight loss of mortar without MSW was nearly the same as that of mortar with MSW, which ranged from 1.5% to 2.0%. Ultimately, mortar with MSW exhibited a lower weight loss at the 700 to 1000 °C temperature. This was due to the increase in weight gain of MSW with temperature. Similarly, Bautista-Marín et al. [43] reported a weight change in MSW heated from 30 to 1100 °C. The results showed that the rate of weight gain increased with temperature, with the maximum gain occurring at 565 °C, indicating oxidation of Fe_3O_4 to Fe_2O_3. In summary, the weight of MSW increased after oxidization, forming Fe_2O_3.

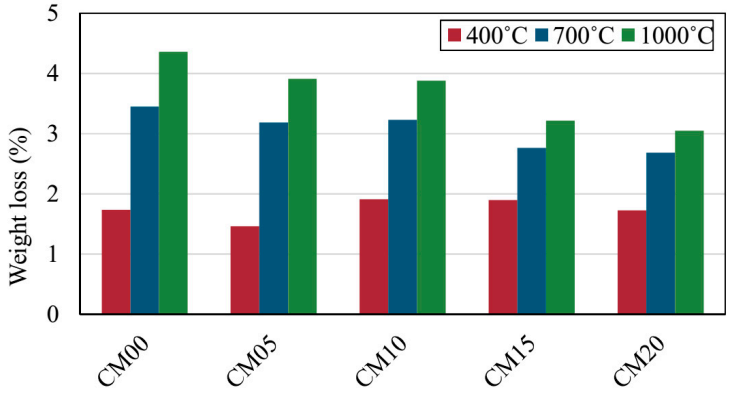


Figure 16. Weight loss of mortar after exposure to elevated temperatures.

3.7.3. Compressive and Residual Strengths

The compressive strength of the mortar was tested at ambient temperature and after exposure to elevated temperatures. The results presented in Figures 17 and 18 illustrate the relationship between residual compressive strength and MSW content at various temperatures, providing a clearer understanding of the impact of elevated temperatures. For specimens of CM00, CM05, CM10, CM15, and CM20 mixes exposed to a temperature of 400 °C, the residual strength values were 83%, 80%, 98%, 95%, and 96%, respectively.

Increasing the amount of MSW in the mortar mixture resulted in a higher residual strength compared to plain cement mortar. Following exposure to temperatures of 700 °C and 1000 °C, the remaining strengths were about 38–45% and 5–20% of the initial strengths, which were 14.3–21.0 MPa and 3.2–7.6 MPa, respectively. These remaining strengths can extend the structure's breakdown after a fire.

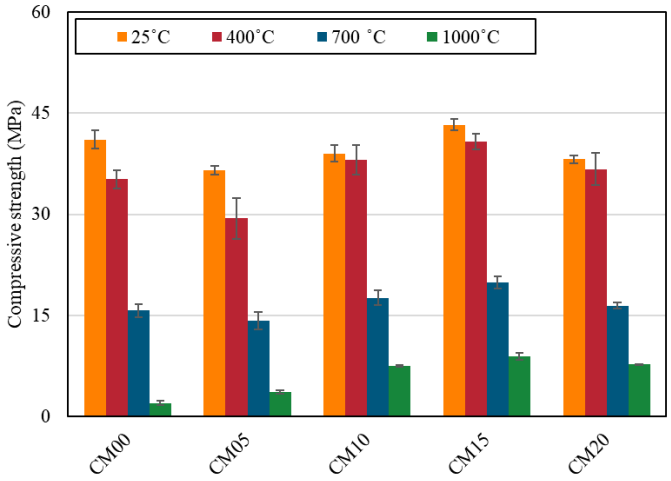


Figure 17. Compressive strength of mortar after exposure to elevated temperatures.

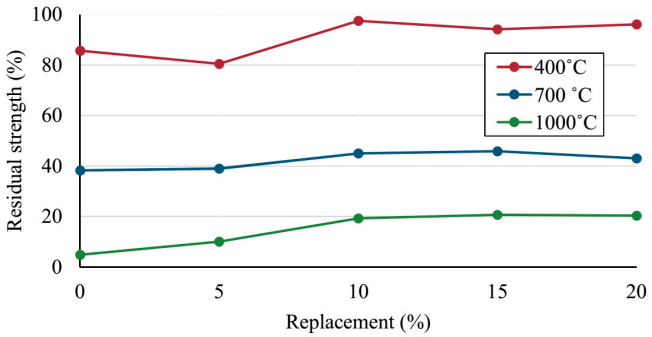


Figure 18. Residual compressive strength of mortar after exposure to elevated temperatures.

This reduction in strength can be attributed to the decomposition of hydration products. Previous research by Lai et al. [44] indicates that the interfacial transition zone (ITZ) between aggregate and cement paste in concrete exhibits enhanced strength as a result of the aggregate's multi-angular shape, rough surface, and porous properties. Nevertheless, the ITZ mostly comprised $Ca(OH)_2$, which initiated decomposition at approximately 350 °C and underwent total decomposition at approximately 530 °C. Therefore, the interfacial transition zone (ITZ) would undergo degradation when exposed to a temperature of 600 °C, resulting in a more significant decline in the strength of concrete [42].

It should be noted that as the MSW content increases, the residual strength of the cement mortar rises compared to plain cement mortar. These findings conformed to those observed at temperatures of 400 °C with an MSW replacement of 10–20%. The increase in porosity and a decrease in the thermal conductivity of mortar containing MSW may reduce pore pressure and a narrower temperature gradient between the core and surface of the specimens [45]. Thus, the addition of MSW enhanced the strength of the mixtures after a fire event.

This study highlights the significance of MSW in improving the residual compressive strength of cement mortar. This enhancement is linked to the ability of vapor to escape through microvoids created by the material's thermal degradation. At this thermal threshold, CM20 displayed greater residual compressive strength than CM00. Figure 19a shows

C-S-H and AFt crystals in CM00 at room temperature. In addition, Figure 19b shows MSW with a thin, flaky texture and distributed pores, along with the interfacial transition zone (ITZ) between the MSW and cement paste.

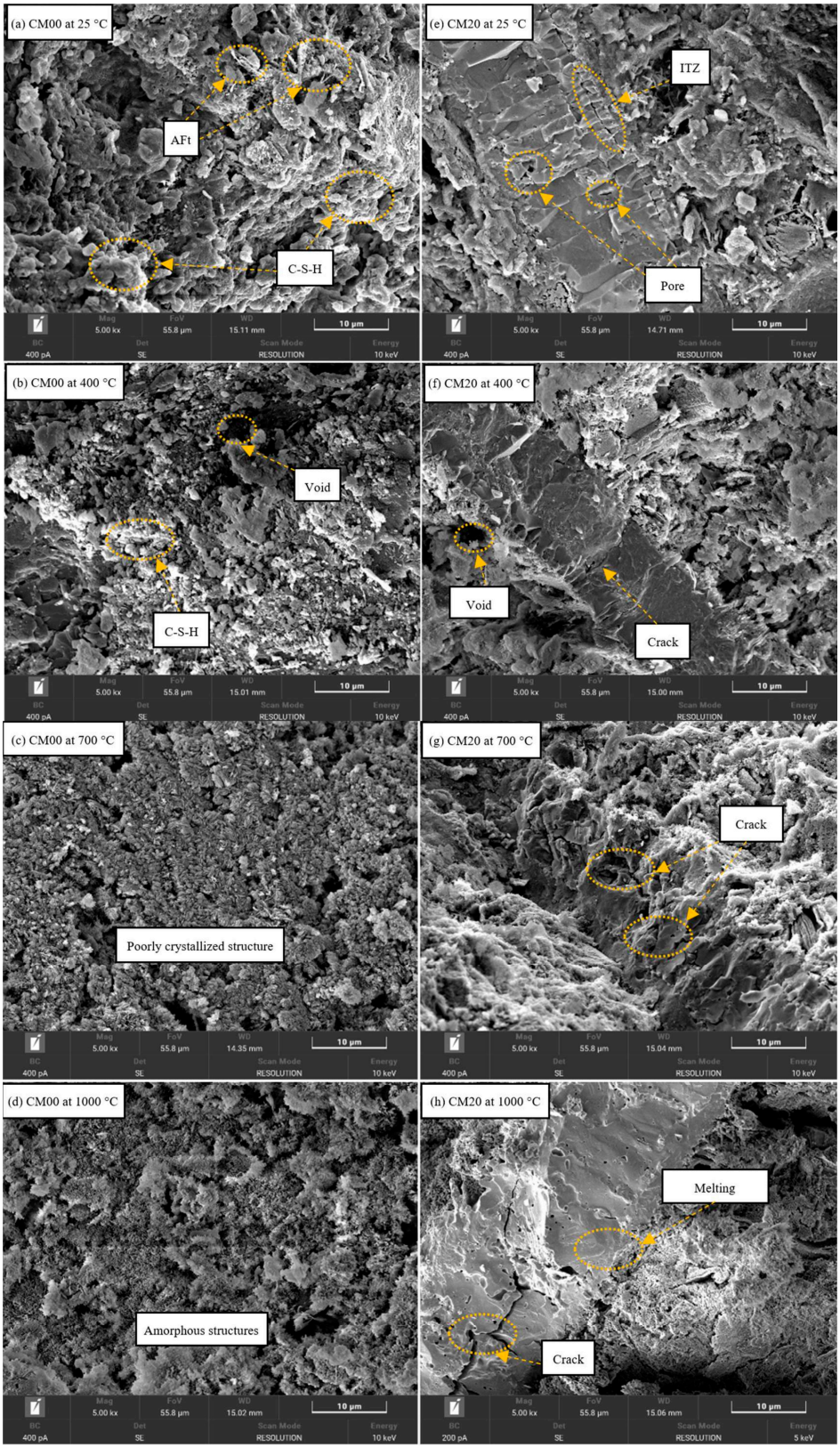


Figure 19. SEM of the core of cement mortar: CM00 (**a**–**d**) and CM20 (**e**–**h**).

At 400 °C, the initial decomposition of the C-S-H structure is observable. As shown in Figure 19b, the C-S-H starts to deteriorate, creating a larger void in the matrix, which contributes to a significant decline in the compressive strength of mortar [46]. Figure 19f shows that the C-S-H structure remains recognizable and retains its morphology and density, indicating that CM20 had higher residual compressive strength compared to CM00.

At 700 °C, the hydration product in CM00 exhibited a poorly crystallized structure (Figure 19c). The cement mortar underwent further degradation, with noticeable discoloration and fissuring on the specimens' surface. As shown in Figure 15, cracks became increasingly evident as the temperature rose to 1000 °C [47,48]. In Figure 19g, the hydration product of CM20 shows greater density than CM00: although CM20 had larger cracks, it retained its structural integrity.

At temperatures of 1000 °C, the microstructural integrity of cement mortar significantly degraded, resulting in amorphous hydration products, as shown in Figure 19d. In contrast, the structural integrity of MSW was sustained at elevated temperatures, though some small cracks were observed (Figure 19h). Some MSW components may develop bonds with C-S-H, leading to greater residual strength compared to CM00 (Figure 19f–h). This increased strength is attributed to the microporous architecture of MSW, which allows for the expulsion of high-pressure water vapor from evaporation, thereby reducing damage [45,49].

4. Conclusions

This paper reports the physical, mechanical, durability, and characteristics of mortars that incorporate mill scale waste (MSW) as natural fine aggregate (NFA) after being subjected to elevated temperatures, with a view to utilizing this waste as construction materials. Based on the experimental results, the main findings can be summarized as follows.

- The use of MSW as NFA replacement resulted in a reduction in workability and thermal conductivity, while the porosity and dry density tended to slightly increase.
- The optimum compressive and flexural strengths were found at 15%vol of MSW as a sand replacement with compressive and flexural strengths at 28 days of 44.1 MPa and 7.2 MPa, respectively.
- The increase in MSW content did not seem to impact the ability to resist acid corrosion. However, it significantly enhanced chloride resistance.
- After being exposed to various temperatures, the use of MSW enhanced the residual compressive strength of the mortar with residual strength of 38–45% and 5–20% for exposure to temperatures of 700 °C and 1000 °C, respectively. In addition, the weight loss exhibited a minimal rise with rising temperature.
- Additionally, the use of MSW as a partial NFA replacement in mortar not only saves landfill space and reduces solid waste but also reduces raw natural material consumption.

Overall, using MSW in mortar mixtures showed several effects, including reduced workability, thermal conductivity, and slightly increased porosity. It enhanced chloride resistance and maintained residual compressive strength even after exposure to high temperatures. The mixture with 15% MSW demonstrated optimal performance, achieving suitable compressive and flexural strengths. These findings indicate that NFA replacement with MSW is a sustainable approach to repurposing waste materials and conserving natural aggregates in construction.

Author Contributions: Conceptualization, A.S. and V.S.; methodology, A.S., A.W. and N.E.-A.; validation, A.W., N.E.-A., P.S. and P.C.; investigation, A.S.; resources, V.S.; data curation, A.S.; writing—original draft preparation, A.S.; writing—review and editing, V.S., P.S. and P.C.; supervision, V.S.; funding acquisition, V.S. All authors have read and agreed to the published version of the manuscript.

Funding: This research was funded by the Fundamental Fund of Khon Kaen University. Research on "the use of heavy weight aggregate in geopolymer composites" has received funding support from the National Science, Research and Innovation Fund (NSRF).

Data Availability Statement: Data will be made available on request.

Conflicts of Interest: The authors declare no conflicts of interest.

References

1. Nidheesh, P.V.; Kumar, M.S. An Overview of Environmental Sustainability in Cement and Steel Production. *J. Clean. Prod.* **2019**, *231*, 856–871. [CrossRef]
2. Remus, R.; Roudier, S.; Aguado-Monsonet, M.A.; Delgado Sancho, L.; Institute for Prospective Technological Studies. *Best Available Techniques (BAT) Reference Document for Iron and Steel Production: Industrial Emissions Directive 2010/75/EU: Integrated Pollution Prevention and Control*; Publications Office: Luxembourg, 2013. [CrossRef]
3. Sharma, R.D.; Singh, N. Evaluation of Strength and Absorption Behaviour of Iron Slag and Recycled Aggregates Concrete and Its Comparative Environmental Estimation by Life Cycle Assessment. *Clean. Mater.* **2023**, *10*, 100210. [CrossRef]
4. Ahmed, S.M.; Kamal, I. Electrical Resistivity and Compressive Strength of Cement Mortar Based on Green Magnetite Nanoparticles and Wastes from Steel Industry. *Case Stud. Constr. Mater.* **2022**, *17*, e01712. [CrossRef]
5. Umadevi, T.; Brahmacharyulu, A.; Karthik, P.; Mahapatra, P.C.; Prabhu, M.; Ranjan, M. Recycling of Steel Plant Mill Scale via Iron Ore Sintering Plant. *Ironmak. Steelmak.* **2012**, *39*, 222–227. [CrossRef]
6. Chousidis, N.; Rakanta, E.; Ioannou, I.; Batis, G. Influence of Iron Mill Scale Additive on the Physico-Mechanical Properties and Chloride Penetration Resistance of Concrete. *Adv. Cem. Res.* **2016**, *28*, 389–402. [CrossRef]
7. Ismail, Z.Z.; AL-Hashmi, E.A. Reuse of Waste Iron as a Partial Replacement of Sand in Concrete. *Waste Manag.* **2008**, *28*, 2048–2053. [CrossRef]
8. Alwaeli, M.; Nadziakiewicz, J. Recycling of Scale and Steel Chips Waste as a Partial Replacement of Sand in Concrete. *Constr. Build. Mater.* **2012**, *28*, 157–163. [CrossRef]
9. Keleştemur, O.; Arıcı, E. Analysis of Some Engineering Properties of Mortars Containing Steel Scale Using Taguchi Based Grey Method. *J. Build. Eng.* **2020**, *29*, 101015. [CrossRef]
10. Velumani, P.; Manikandan, P. Steel Mill Scale Waste and Granite Powder Waste in Concrete Production—An Experimental Study. *Mater. Today Proc.* **2020**, *37*, 1748–1752. [CrossRef]
11. *ASTM C128-22*; Standard Test Method for Relative Density (Specific Gravity) and Absorption of Fine Aggregate. ASTM International: West Conshohocken, PA, USA, 2022.
12. *ASTM C 136-06*; Standard Test Method for Sieve Analysis of Fine and Coarse Aggregates. ASTM International: West Conshohocken, PA, USA, 2006.
13. *ASTM C33/C33M-11*; Standard Specification for Concrete Aggregates. ASTM International: West Conshohocken, PA, USA, 2011.
14. *ASTM C305-11*; Standard Practice for Mechanical Mixing of Hydraulic Cement Pastes and Mortars of Plastic Consistency. ASTM International: West Conshohocken, PA, USA, 2011.
15. *ASTM C1437-07*; Standard Test Method for Flow of Hydraulic Cement Mortar. ASTM International: West Conshohocken, PA, USA, 2007.
16. *ASTM C109/C109M-13*; Standard Test Method for Compressive Strength of Hydraulic Cement Mortars (Using 2-in. or [50-Mm] Cube Specimens). ASTM International: West Conshohocken, PA, USA, 2013.
17. *ASTM C642-13*; Standard Test Method for Density, Absorption, and Voids in Hardened Concrete. ASTM International: West Conshohocken, PA, USA, 2013.
18. *ASTM C267-12*; Standard Test Methods for Chemical Resistance of Mortars, Grouts, and Monolithic Surfacings and Polymer Concretes. ASTM International: West Conshohocken, PA, USA, 2012.
19. *ASTM C348-22*; Standard Test Method for Flexural Strength of Hydraulic-Cement Mortars. ASTM International: West Conshohocken, PA, USA, 2022.
20. *ASTM C597-08*; Standard Test Method for Ultrasonic Pulse Velocity Through Concrete. ASTM International: West Conshohocken, PA, USA, 2008.

21. Wongkvanklom, A.; Posi, P.; Kasemsiri, P.; Sata, V.; Cao, T.; Chindaprasirt, P. Strength, Thermal Conductivity and Sound Absorption of Cellular Lightweight High Calcium Fly Ash Geopolymer Concrete. *Eng. Appl. Sci. Res.* **2021**, *48*, 487–496. [CrossRef]
22. *ASTM D5930-09*; Standard Test Method for Thermal Conductivity of Plastics by Means of a Transient Line-Source Technique. ASTM International: West Conshohocken, PA, USA, 2009.
23. Otsuki, N.; Nagataki, S.; Nakashita, K. Evaluation of the $AgNO_3$ Solution Spray Method for Measurement of Chloride Penetration into Hardened Cementitious Matrix Materials. *Constr. Build. Mater.* **1993**, *7*, 195–201. [CrossRef]
24. Ghosh, P.; Tran, Q. Correlation Between Bulk and Surface Resistivity of Concrete. *Int. J. Concr. Struct. Mater.* **2015**, *9*, 119–132. [CrossRef]
25. Wongsa, A.; Sata, V.; Nuaklong, P.; Chindaprasirt, P. Use of Crushed Clay Brick and Pumice Aggregates in Lightweight Geopolymer Concrete. *Constr. Build. Mater.* **2018**, *188*, 1025–1034. [CrossRef]
26. Murthy, Y.I. On The Mechanical Aspects Concrete Containing Mill Scale. *Int. J. Civ. Eng.* **2021**, *8*, 23–34. [CrossRef]
27. Ganeshprabhu, P.; Chandrasekaran, P.; Sheerin Farzana, A. Engineering Behaviour of Sustainable Concrete with Steel Mill Scale. *Polish J. Environ. Stud.* **2021**, *30*, 1129–1137. [CrossRef]
28. Ozturk, M.; Depci, T.; Bahceci, E.; Karaaslan, M.; Akgol, O.; Sevim, U.K. Production of New Electromagnetic Wave Shielder Mortar Using Waste Mill Scales. *Constr. Build. Mater.* **2020**, *242*, 118028. [CrossRef]
29. Koronthalyova, O.; Matiasovsky, P. Thermal Conductivity of Fibre Reinforced Porous Calcium Silicate Hydrate-Based Composites. *J. Build. Phys.* **2003**, *27*, 71–89. [CrossRef]
30. Lima, W.M.; Biondo, V.; Weinand, W.R.; Nogueira, E.S.; Medina, A.N.; Baesso, M.L.; Bento, A.C. The Effect of Porosity on Thermal Properties: Towards a Threshold of Particle Contact in Sintered Stainless Steel. *J. Phys. Condens. Matter* **2005**, *17*, 1239–1249. [CrossRef]
31. Vincent, C.; Silvain, J.F.; Heintz, J.M.; Chandra, N. Effect of Porosity on the Thermal Conductivity of Copper Processed by Powder Metallurgy. *J. Phys. Chem. Solids* **2012**, *73*, 499–504. [CrossRef]
32. Wang, J.; Carson, J.K.; North, M.F.; Cleland, D.J. A New Approach to Modelling the Effective Thermal Conductivity of Heterogeneous Materials. *Int. J. Heat Mass Transf.* **2006**, *49*, 3075–3083. [CrossRef]
33. Sornlar, W.; Wannagon, A.; Supothina, S. Stabilized Homogeneous Porous Structure and Pore Type Effects on the Properties of Lightweight Kaolinite-Based Geopolymers. *J. Build. Eng.* **2021**, *44*, 103273. [CrossRef]
34. Furlani, E.; Maschio, S. Steel Scale Waste as Component in Mortars Production: An Experimental Study. *Case Stud. Constr. Mater.* **2016**, *4*, 93–101. [CrossRef]
35. Bilir, T.; Gencel, O.; Topcu, I.B. Properties of Mortars with Fly Ash as Fine Aggregate. *Constr. Build. Mater.* **2015**, *93*, 782–789. [CrossRef]
36. Moura, M.A.N.; Júnior, A.L.M.; Ferreira, G.C.S. Ultrasonic Testing on Evaluation of Concrete Residual Compressive Strength: A Review. *Constr. Build. Mater.* **2023**, *373*, 130887. [CrossRef]
37. Nuaklong, P.; Sata, V.; Chindaprasirt, P. Properties of Metakaolin-High Calcium Fly Ash Geopolymer Concrete Containing Recycled Aggregate from Crushed Concrete Specimens. *Constr. Build. Mater.* **2018**, *161*, 365–373. [CrossRef]
38. Parvathikumar, G.; Sahadevan, B.; Palanisamy, C. Scrap Steel Mill Scale as River Sand Replacement in Cement Concrete: Effect on Durability Characteristics. *J. Mater. Cycles Waste Manag.* **2024**, *26*, 1490–1504. [CrossRef]
39. Christensen, B.J.; Christensen, B.J.; Coverdale, R.T.; Coverdale, R.T.; Olson, R.A.; Olson, R.A.; Ford, S.J.; Ford, S.J.; Garboczi, E.J.; Garboczi, E.J.; et al. Impedance Spectroscopy of Hydrating Cement-Based Materials: Measurement, Interpretation, and Application. *J. Am. Ceram. Soc.* **1994**, *77*, 2789–2804. [CrossRef]
40. Horňáková, M.; Lehner, P. Relationship of Surface and Bulk Resistivity in the Case of Mechanically Damaged Fibre Reinforced Red Ceramic Waste Aggregate Concrete. *Materials* **2020**, *13*, 5501. [CrossRef] [PubMed]
41. Short, N.R.; Purkiss, J.A.; Guise, S.E. Assessment of Fire Damaged Concrete Using Colour Image Analysis. *Constr. Build. Mater.* **2001**, *15*, 9–15. [CrossRef]
42. Ho, J.C.M.; Liang, Y.; Wang, Y.H.; Lai, M.H.; Huang, Z.C.; Yang, D.; Zhang, Q.L. Residual Properties of Steel Slag Coarse Aggregate Concrete after Exposure to Elevated Temperatures. *Constr. Build. Mater.* **2022**, *316*, 125751. [CrossRef]
43. Bautista-Marín, J.D.; Esguerra-Arce, A.; Esguerra-Arce, J. Use of an Industrial Solid Waste as a Pigment in Clay Bricks and Its Effects on the Mechanical Properties. *Constr. Build. Mater.* **2021**, *306*, 124848. [CrossRef]
44. Lai, M.H.; Zou, J.; Yao, B.; Ho, J.C.M.; Zhuang, X.; Wang, Q. Improving Mechanical Behavior and Microstructure of Concrete by Using BOF Steel Slag Aggregate. *Constr. Build. Mater.* **2021**, *277*, 122269. [CrossRef]
45. Nuaklong, P.; Boonchoo, N.; Jongvivatsakul, P.; Charinpanitkul, T.; Sukontasukkul, P. Hybrid Effect of Carbon Nanotubes and Polypropylene Fibers on Mechanical Properties and Fire Resistance of Cement Mortar. *Constr. Build. Mater.* **2021**, *275*, 122189. [CrossRef]
46. Wang, Y.; Fu, C.; Kuang, H.; Qin, H.; Xu, T.; Meng, W. Experimental Study on the Mechanical Properties of Cement-Based Grouting Materials after Exposed to High Temperatures. *Case Stud. Constr. Mater.* **2024**, *20*, e03068. [CrossRef]

47. Zhu, H.; Wu, Q.; Zhang, C.; Deng, F. Thermal Stability and Structural Characterization of Class G Oil Well Cement Paste Exposed to Elevated Temperature. *J. Mater. Civ. Eng.* **2015**, *27*, 04015014. [CrossRef]
48. Ogrodnik, P.; Rutkowska, G.; Powęzka, A.; Żółtowski, M.; Szulej, J.; Wiśniewski, K.; Howorus, P. Research on the Effect of Fire Thermal Energy on the Microstructure and Properties Mechanical of Fiber-Reinforced Cement Mortars. *Energies* **2023**, *16*, 6450. [CrossRef]
49. Sedaghatdoost, A.; Behfarnia, K. Mechanical Properties of Portland Cement Mortar Containing Multi-Walled Carbon Nanotubes at Elevated Temperatures. *Constr. Build. Mater.* **2018**, *176*, 482–489. [CrossRef]

Disclaimer/Publisher's Note: The statements, opinions and data contained in all publications are solely those of the individual author(s) and contributor(s) and not of MDPI and/or the editor(s). MDPI and/or the editor(s) disclaim responsibility for any injury to people or property resulting from any ideas, methods, instructions or products referred to in the content.